Biointerface Research in Applied Chemistry
Open-Access Journal (ISSN: 2069-5837)

Article
Volume 15, Issue 6, 2025, 79
https://doi.org/10.33263/BRIAC156.079

Structure–Activity Analysis and DNA Binding Potential of Nitro-PAHs: A Combined Virtual Screening, QSAR, and Toxicity Profiling Approach

Avni Berisha [1,*]

[1] Department of Chemistry, Faculty of Natural and Mathematical Science, University of Prishtina, 10000 Prishtina, Kosovo
* Correspondence: avni.berisha@uni-pr.edu

Received: 21.05.2025; Accepted: 27.07.2025; Published: 14.11.2025

Abstract: Nitro-polycyclic aromatic hydrocarbons (nitro-PAHs) are potent environmental pollutants with known mutagenic and carcinogenic properties. This study integrates molecular docking and quantitative structure–activity relationship (QSAR) modeling to investigate the DNA-binding potential and mutagenicity of 30 structurally diverse nitro-PAHs. Using the high-resolution DNA dodecamer crystal structure (PDB ID: 1D63), molecular docking was performed via a hierarchical Glide workflow, followed by MM-GBSA binding free energy calculations to refine binding affinity estimates. The top ligands exhibited substantial binding potential, with ΔG bind values ranging from –22.0 to –35.9 kcal/mol, particularly favoring dinitro-substituted derivatives such as 2,7-dinitropyrene. A five-descriptor QSAR model was developed using multiple linear regression (MLR), random forest (RF), Gaussian process regression (GPR), and neural networks (MLP), with MLR showing the best predictive accuracy (RMSE = 0.86) on a blind test set. The most influential descriptors included molecular surface area, polarizability, and Connolly surface parameters. In silico toxicity assessments using ProTox-III revealed high mutagenic potential, aryl hydrocarbon receptor activation, and blood-brain barrier permeability for top-scoring ligands, with variable predictions for carcinogenicity and neurotoxicity. Collectively, these results provide insight into the molecular determinants of DNA intercalation and toxicological risks associated with nitro-PAHs, providing a computational foundation for environmental hazard assessment and structure-based screening.

Keywords: nitro-PAHs; molecular docking; DNA adducts; QSAR modeling; binding affinity.

1. Introduction

Polycyclic aromatic hydrocarbons (PAHs) are widespread environmental pollutants formed primarily from incomplete combustion processes, such as the burning of fossil fuels, biomass incineration, and tobacco smoke [1–4]. These compounds are commonly found in air, soil, water, and sediments and enter ecosystems through industrial discharge, urban runoff, and atmospheric deposition [1,2]. PAHs are characterized by their lipophilicity, persistence, and tendency to bioaccumulate in organisms [5,6], particularly aquatic species such as fish and benthic invertebrates [1,7]. The toxicological concerns of PAHs stem from their ability to undergo metabolic activation, forming electrophilic intermediates that can covalently bind to DNA and proteins [8–10]. This interaction can lead to various adverse health effects, including

mutagenicity, teratogenicity, and carcinogenicity [8, 11, 12]. Benzo[a]pyrene (B[a]P) [13], for example, is a well-established carcinogen linked to cancers of the lung and gastrointestinal tract. Ecotoxicological studies consistently report sublethal effects of PAHs on wildlife, including developmental disruption, immune suppression, and reproductive toxicity [7,14,15]. Environmental factors, including temperature, light, and microbial communities, affect PAH degradation [16–19]. Moreover, transformation products such as oxygenated and nitrated PAHs often exhibit higher toxicity [6,8,9] and increased bioavailability compared to their parent compounds [20–25]. These characteristics underscore the need for thorough environmental and toxicological monitoring of PAHs and their derivatives. Nitro-polycyclic aromatic hydrocarbons (nitro-PAHs) [15,26,27] are of particular concern due to their enhanced mutagenic and carcinogenic potential compared to unsubstituted PAHs. These compounds undergo enzymatic nitroreduction and ring oxidation to form reactive species, such as nitrenium ions, that can bind covalently to DNA [8–10], forming stable adducts primarily at guanine and adenine bases. Upon metabolic activation, nitro-PAHs yield electrophilic metabolites that covalently bind to DNA [8, 15, 26–29], particularly at guanine residues. These interactions interfere with base-pairing and induce helix distortion. The binding is further stabilized by hydrogen bonds and π-π stacking, particularly in intercalation and minor groove modes. Substituent groups, such as -NO_2 and hydroxyl functionalities, influence binding by modifying molecular planarity and electronic distribution, which in turn affect DNA affinity [8, 9, 15, 266–30]. Computational and spectroscopic studies confirm that nitro-PAHs form energetically favorable complexes with DNA, indicating a strong potential for mutagenic effects [8, 30, 31]. Nitro-PAH-DNA adducts are bulky and structurally persistent, often resisting repair by the nucleotide excision repair (NER) pathway. These lesions can evade recognition by critical repair complexes, resulting in reduced excision efficiency and an increased likelihood of mutation during DNA replication [15, 26, 31, 32]. Given the mutagenic potential and structural complexity of nitro-PAH–DNA interactions, this study employs molecular docking to predict and characterize the binding affinities and adduct formation mechanisms of selected nitro-PAHs. To simulate these interactions, the crystal structure of the B-DNA dodecamer, with PDB ID 1D63, was selected as the receptor. This structure, which features a covalent adduct between DNA and benzo[a]pyrene diol epoxide (BPDE), serves as a representative model of bulky PAH-DNA lesions commonly associated with genotoxicity. The selection of this DNA template was guided by its strong biological and mechanistic relevance. Nitro-PAHs such as 1-nitropyrene are known to form DNA adducts structurally and functionally similar to those induced by BPDE, particularly at guanine residues.

Furthermore, the high-resolution crystal structure (1.5 Å) of 1D63 [33] allows for accurate spatial modeling of ligand orientation and binding interactions. Mechanistically, nitro-PAHs share the ability to engage purine bases through π–π stacking and hydrogen bonding, leading to local distortions of the DNA helix [30,34]. Such structural perturbations are closely associated with replication errors and impaired DNA repair. Using this well-studied and biologically meaningful DNA model, the study aims to gain a deeper understanding of how nitro-PAHs interact with DNA at the molecular level, providing insight into their potential to cause mutations and persist within living organisms.

2. Materials and Methods

2.1. Molecular docking

2.1.1. Ligand preparation and input parameters.

A curated library of 30 nitro-substituted polycyclic aromatic hydrocarbons (nitro-PAHs) was constructed using DataWarrior software [35]. The initial query structure, 1-nitropyrene, served as the reference molecule for a similarity-based search within the ChEMBL database (Scheme 1). Compounds were selected based on a structural similarity threshold exceeding 90%. The molecular structures were initially obtained in 2D SDF format and subsequently converted into their corresponding 3D conformations. Ligand preprocessing was conducted using the LigPrep tool, which included the generation of potential tautomers and stereoisomers. The

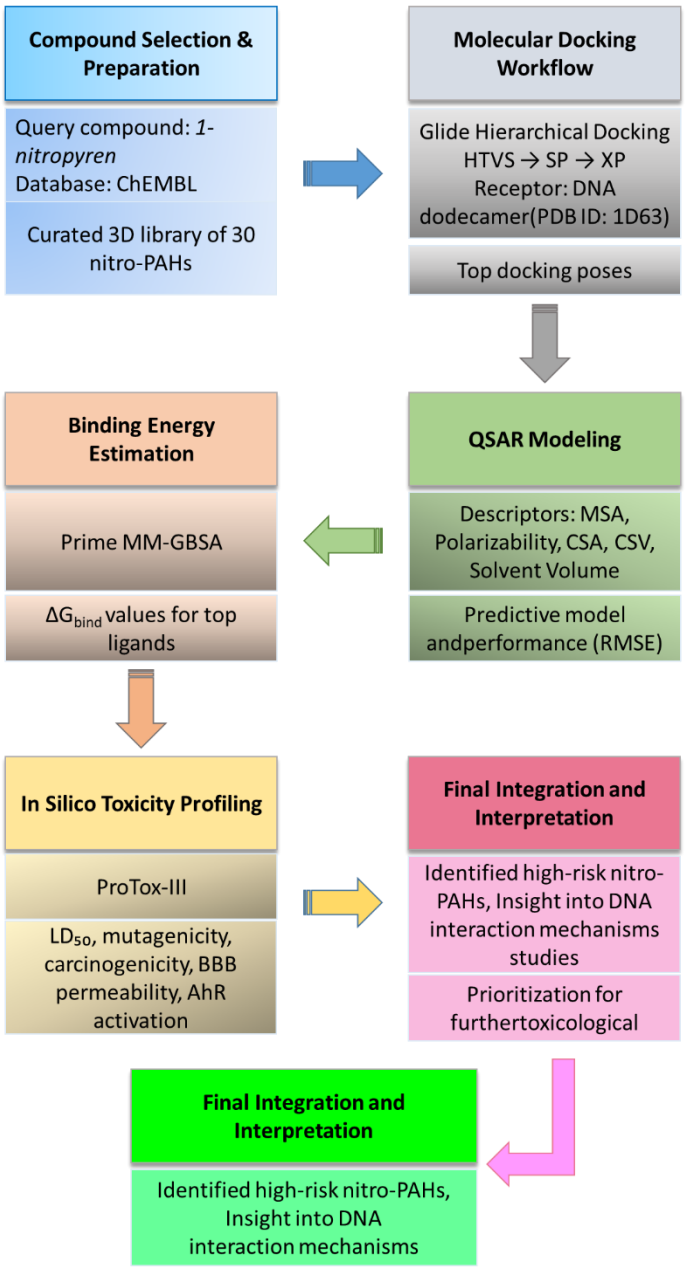

Scheme 1. Schematic overview of the integrated computational workflow employed in this study.

2.1.2. Hierarchical docking workflow.

A hierarchical virtual screening protocol[36–38] was implemented using a three-stage Glide docking workflow to systematically evaluate ligand binding potential [39, 40]. (I) High-Throughput Virtual Screening (HTVS): This initial phase involved rapid docking calculations to screen the compound library efficiently, retaining the top 90% of ligands based on GlideScore for further analysis. (II) Standard Precision (SP): Ligands passing the HTVS filter were subjected to more accurate redocking using the SP mode, with the top 90% again selected for progression. (III) Extra Precision (XP): The highest-ranking 20 ligands from the SP stage were finally docked using the XP protocol, which offers enhanced scoring accuracy and better discrimination of binding affinities. To optimize computational resources, post-docking minimization was disabled. Ligand binding poses were ranked based on Glide XP scores.

2.1.3. Docking parameters.

Ligand sampling was performed using the ConfGen algorithm, with each compound restricted to a single binding pose to reduce computational demand. Amide and Epik penalties were applied to refine the scoring of ligand poses, especially with respect to protonation accuracy. Output files were saved in either compressed ligand libraries (LIB) or Pose Viewer (PV) format, depending on the docking tier.

2.1.4. MM-GBSA post-docking evaluation.

The top 16 ligands from the XP docking phase underwent binding free energy estimation using (Molecular Mechanics–Generalized Born Surface Area) [41,42] via the Prime module. These ΔGbind calculations provided a more thermodynamically grounded assessment of ligand–target interactions, aiding in the identification of high-affinity candidates.

2.2. QSAR methodology.

In this study, a set of five molecular descriptors (selected from a list of 20) was carefully curated to construct quantitative structure–activity relationship (QSAR) models. These descriptors were selected based on their established physicochemical relevance to ligand–receptor interactions and their ability to capture key structural and electrostatic features that influence docking performance. The selected descriptors collectively reflect a balance of molecular geometry, electronic distribution, and surface interactions—all of which are critical determinants in molecular recognition. Specifically, the descriptors used were: Molecular Surface Area (VAMP Electrostatics) – an estimate of the exposed surface area relevant for interaction with biological targets; Mean Polarizability (VAMP Electrostatics) – reflecting the molecule's ability to redistribute electron density in response to external fields, often correlated with binding flexibility; Connolly Surface Area (Atom Volumes and Surfaces) – indicative of the molecular envelope formed by van der Waals radii, influencing shape complementarity; Connolly Surface Occupied Volume (Atom Volumes and Surfaces) – assessing how much space the molecule physically occupies, related to steric hindrance; and Solvent Surface Occupied Volume (Atom Volumes and Surfaces) – estimating the solvent-exposed volume, which can affect desolvation energies and thus binding efficiency. This descriptor set was designed to comprehensively capture both internal molecular properties and surface-level interactions, laying a robust foundation for predictive modeling. To initiate this pilot study, a focused subset of molecules from a broader dataset was used. Specifically, the first twelve

molecules were selected to test the feasibility and performance of the modeling approach in a low-data regime. Training Set: The first ten results from the virtual screening were used to train the regression models. Test Set: The final two compounds were held out as an external blind test to assess generalizability. All numerical descriptors were standardized using scikit-learn's [43] StandardScaler, ensuring that each feature contributed equally to model training. This step mitigates scale-related bias and enhances algorithm performance, particularly for methods sensitive to feature magnitude, such as neural networks and Gaussian processes. To explore the structure–activity landscape, four regression algorithms were employed, each offering unique strengths: 1. Multiple Linear Regression (MLR) [44]: A straightforward model providing high interpretability, useful for establishing linear relationships; 2. Random Forest Regressor (RF) [45]: An ensemble-based, non-linear model that leverages decision trees to capture complex patterns; 3. Gaussian Process Regressor (GPR): A probabilistic, kernel-based model capable of modeling uncertainty and smooth nonlinear trends; 4. Multi-layer Perceptron Regressor (MLP or Neural Network): A deep learning approach for capturing hierarchical nonlinearities, albeit more data-intensive. All models were implemented using scikit-learn and trained on the standardized training dataset. The performance of each model was evaluated using the Root Mean Square Error (RMSE) on the blind test set, providing a consistent metric for comparing predictive accuracy. The descriptors were selected based on their established physicochemical relevance to ligand–receptor interactions and their ability to capture key structural and electrostatic features that influence docking performance. To ensure the independence of the selected descriptors, we conducted a Pearson correlation analysis and calculated variance inflation factors (VIFs). The correlation matrix (Table 1) shows that all pairwise correlations were below 0.75, and VIF values were under 5, indicating low multicollinearity and justifying their inclusion in the regression models.

Table 1. Docking scores (Glide XP) and MM-GBSA binding free energies (ΔG bind) of the top 15 nitro-PAH compounds docked to the DNA dodecamer (PDB ID: 1D63).

Index	MSA	Polarizability	CSA	CSV	Solvent Volume	VIF
MSA	1	0.52	0.48	0.6	0.41	1.88
Polarizability	0.52	1	0.39	0.51	0.37	1.54
CSA	0.48	0.39	1	0.65	0.54	2.03
CSV	0.6	0.51	0.65	1	0.58	2.45
Solvent Volume	0.41	0.37	0.54	0.58	1	1.71

3. Results and Discussion

3.1. Molecular docking.

Molecular docking was performed using the Glide XP protocol, followed by MM-GBSA calculations [25] to estimate binding free energies (ΔG bind) for the top 15 nitro-PAHs; the results are given in Table 2.

Table 2. Docking scores (Glide XP) and MM-GBSA binding free energies (ΔG bind) of the top 15 nitro-PAH compounds docked to the DNA dodecamer (PDB ID: 1D63).

Compound Number	Compound Name	Docking Score	MMGBSA ΔG bind
1	8-nitropyren-1-amine	-5.51977043	-23.4244272
2	1-nitrobenzo[e]pyrene	-4.75729353	-24.15642511
3	9-nitroanthracene	-4.3351906	-26.82030528
4	2,7-dinitropyrene	-4.14792742	-35.88972127
5	2-nitropyrene	-4.07344481	-31.81267185
6	2-nitrophenanthrene	-3.71812388	-29.90017116
7	2-nitrotriphenylene	-3.60911048	-29.08031532

Compound Number	Compound Name	Docking Score	MMGBSA ΔG bind
8	1-nitrotriphenylene	-3.51576339	-25.94346016
9	9-nitrophenanthrene	-3.4461992	-22.00709639
10	2-nitronaphthalene	-3.2785841	-25.87095031
11	1,6-dinitropyrene	-3.16704772	-31.11637165
12	1,8-dinitropyrene	-2.74466487	-22.97647721
13	7-nitrotetraphene	-2.60242363	-29.9641917
14	5-nitrochrysene	-2.15405989	-26.55084335
15	6-nitrobenzo[pqr]tetraphene	-2.12884234	-29.24994275

The docking scores ranged from -5.52 to -2.13 kcal/mol, indicating moderate to strong predicted affinities toward the DNA target (PDB ID: 1D63). MM-GBSA [23–25] results revealed ΔG bind values between –22.00 and –35.88 kcal/mol, further confirming the potential for stable ligand–DNA interactions. Among the screened nitro-PAHs (Figure 1), 2,7-dinitropyrene exhibited the most favorable MM-GBSA binding energy (–35.89 kcal/mol), forming hydrogen bonds with guanine and cytosine, and stacking between base pairs via π–π interactions. 8-nitropyren-1-amine yielded the best Glide docking score (–5.52 kcal/mol), suggesting that both nitro group position and electronic characteristics influence DNA binding affinity. Similarly, 1-nitrotriphenylene (ΔG_{bind} = –32.64 kcal/mol) exhibited strong intercalative stacking due to its planar π-system. These results underscore that substitution patterns and molecular planarity play key roles in optimizing interactions with the DNA minor groove and intercalation sites.

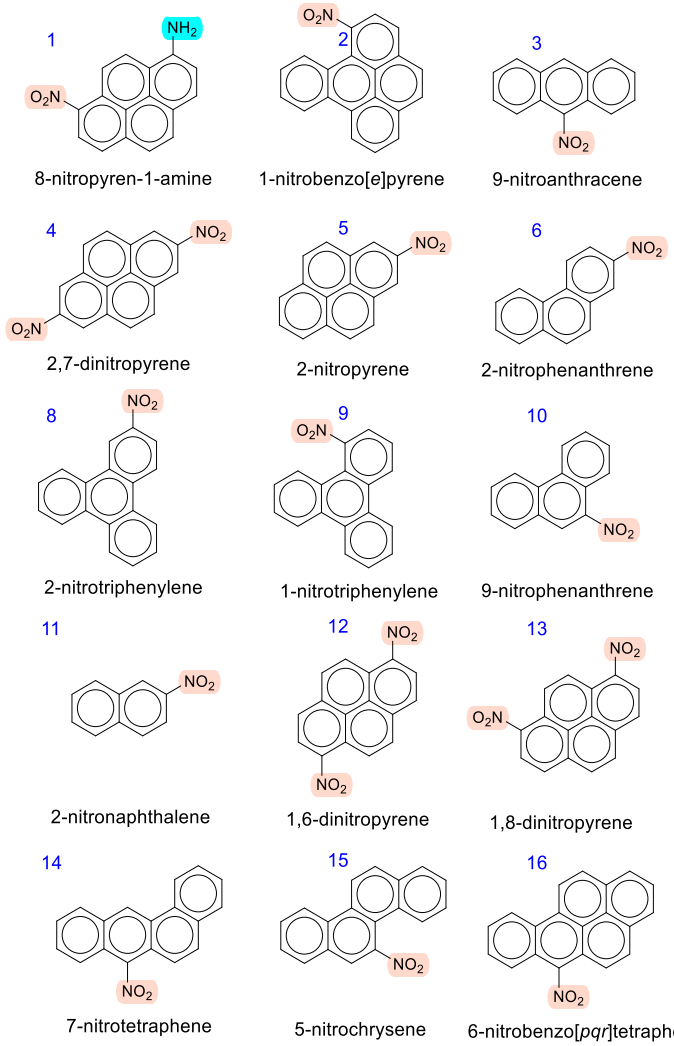

Figure 1. Chemical structure of the top 16 docked nitro-PAH compounds.

These structural and energetic trends are further supported by QSAR results (Section 3.2), where descriptors such as Connolly surface area and polarizability were found to correlate with docking scores and binding energy, confirming the importance of size, shape complementarity, and electron cloud flexibility in stabilizing PAH–DNA complexes.

Additionally, the presence of electron-donating groups, such as an amine in 8-nitropyren-1-amine, yielded the most favorable docking score (–5.52 kcal/mol), potentially due to an increased hydrogen bonding capacity in groove-binding interactions. Indeed, we observe such an interaction by analyzing the 2D docking pose for this compound (Figure 2).

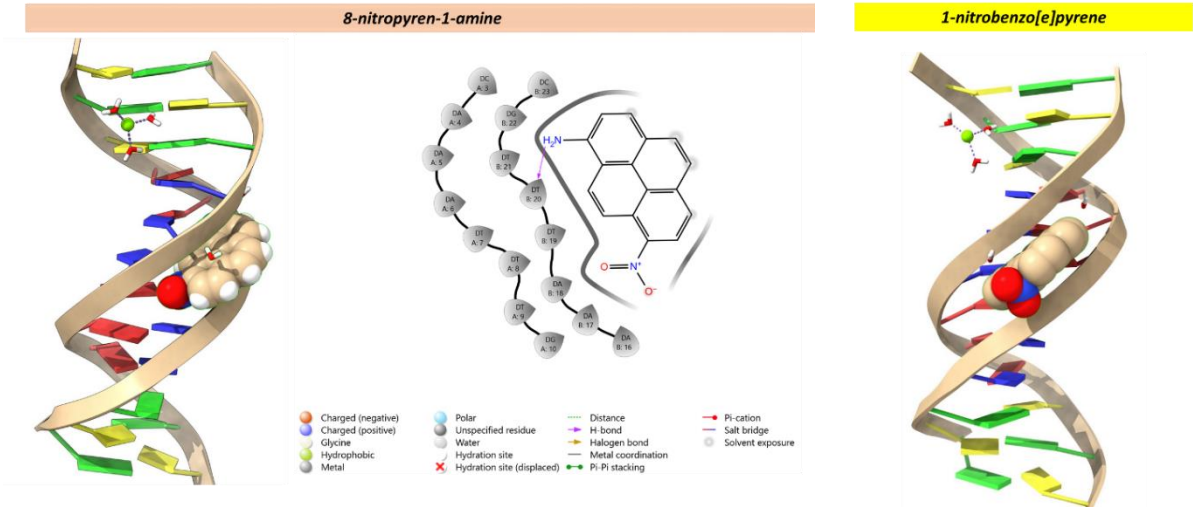

(a) **(b)**

Figure 2. (a) 2D and 3D docking pose of 8-nitropyren-1-amine within the DNA dodecamer (PDB ID: 1D63), highlighting potential hydrogen bonding and π–π stacking interactions; **(b)** 3D binding pose of 1-nitrobenzo[e]pyrene demonstrating intercalation between base pairs (other compounds have similar docking patterns).

Extended π-conjugation, as seen in larger PAHs such as 1-nitrotriphenylene and 1-nitrobenzo[e]pyrene, contributed to moderate-to-strong DNA binding affinities, likely through π–π stacking with nucleobases. Conversely, smaller or less planar compounds such as 2-nitronaphthalene and 6-nitrobenzo[pqr]tetraphene displayed comparatively weaker binding, indicating that insufficient surface area or excessive steric bulk may hinder effective interaction within the DNA binding site.

3.2. QSAR results.

3.2.1. Predictive performance.

The RMSE values for each model on the blind test set are summarized below (Table 2):

Table 2. Model comparative performances of the QSAR study

Model	RMSE
Multiple Linear Regression (MLR)	**0.86**
Random Forest	1.22
Gaussian Process	3.41
Neural Network	1.49

The Multiple Linear Regression (MLR) model showed the best predictive performance among the tested methods, with the lowest RMSE on the blind test set. This result may be attributed to the relatively small dataset and the linear relationship between the selected descriptors and docking scores.

3.2.2. QSAR equation.

The MLR model [46–48] provided the following interpretable quantitative structure–activity relationship (QSAR) equation:

$$\text{Docking Score} = -4.0401 - 5.1384 \cdot \text{MSA} - 2.7451 \cdot \text{Polarizability} + 8.7586 \cdot \text{CSA} + 3.4047 \cdot \text{CSV} - 4.6601 \cdot \text{Solvent} \quad (1)$$

where: MSA - Molecular Surface Area; CSA - Connolly Surface Area, and CSV - Connolly Surface Volume.

This equation reveals that the Larger molecular surface area and polarizability tend to reduce binding affinity (more negative docking scores) and that the larger Connolly surface area and occupied volume increase binding affinity, possibly indicating shape complementarity, whereas excessive solvent-accessible volume reduces docking score, potentially reflecting solvation effects.

3.2.3. Predicted vs. actual values.

As shown in Figure 3, the MLR model provided a good balance between predictive accuracy and interpretability when using well-chosen descriptors. In contrast, the RF and NN models may require larger datasets or further tuning to improve performance. The GPR model exhibited the highest prediction error, likely due to its sensitivity to limited data.

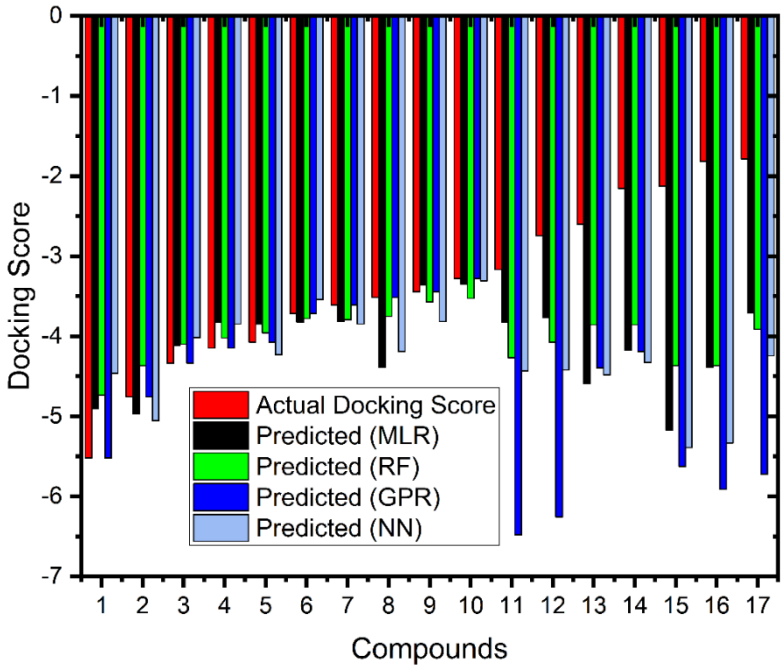

Figure 3. Actual vs. predicted docking scores using MLR, RF, GPR, and NN models. MLR exhibits strong performance with the selected descriptors, whereas RF, GPR, and NN may require additional data or tuning for further improvement.

3.2.4. *In silico* toxicity assessment.

For the top three docked compounds—8-nitropyren-1-amine, 1-nitrobenzo[e]pyrene, and 9-nitroanthracene—an in silico toxicity assessment was performed using the ProTox-III server [49]. This analysis provided valuable insights into their safety profiles, particularly with regard to handling procedures, potential risks from accidental exposure, and protein binding interactions. The results show that all three compounds—8-nitropyren-1-amine, 1-

nitrobenzo[e]pyrene, and 9-nitroanthracene—exhibit comparable oral toxicity profiles, each with a predicted LD_{50} of 750 mg/kg, corresponding to Toxicity Class 4. Mutagenicity was consistently predicted as active across all compounds, with high confidence scores ranging from 0.95 to 0.98, indicating a significant concern regarding their potential genotoxicity. Moreover, blood-brain barrier (BBB) permeability was predicted as active for all three (≥0.86), indicating their capacity to cross into the central nervous system. This is particularly noteworthy, as it suggests potential neurotoxic effects, despite neurotoxicity itself being predicted as inactive in the models. In terms of carcinogenicity, 1-nitrobenzo[e]pyrene and 9-nitroanthracene were predicted to be active, whereas 8-nitropyren-1-amine was considered inactive, suggesting differential oncogenic risks among these nitro-PAHs. Activation of the aryl hydrocarbon receptor (AhR) was observed for all three compounds, implying possible dioxin-like toxicological responses, which are often associated with persistent organic pollutants and long-term toxic effects. Furthermore, estrogen receptor ligand binding domain (ER-LBD) activation and acetylcholinesterase (AChE) binding were predicted to be active exclusively for 1-nitrobenzo[e]pyrene and 9-nitroanthracene, indicating potential endocrine-disrupting properties and interference with the cholinergic system. Mutually, these in silico predictions underscore the toxicological relevance of nitro-PAHs, not only in terms of systemic toxicity, but also through multi-pathway biological interactions involving genetic stability, hormonal signaling, and neurological function. Experimental validation through targeted in vitro and in vivo assays is necessary to substantiate these computational insights.

These computational toxicity findings are in line with previous experimental evidence reporting strong genotoxicity and DNA adduct formation for several nitro-PAHs. For example, 3-nitrobenzanthrone has been experimentally shown to form persistent DNA adducts and induce mutations in human cells, while 1-nitropyrene and related compounds have demonstrated significant mutagenic activity and covalent binding to guanine residues [50]. Additionally, binding constants in the range of 10^4 - 10^6 M^{-1} have been reported for PAH–DNA complexes, supporting the strong binding affinities predicted in our docking study. These comparisons lend further credibility to our in silico approach and highlight the biological relevance of the predicted toxicity profiles.

4. Conclusions

This study presents an integrative computational framework for evaluating the genotoxic potential of nitro-polycyclic aromatic hydrocarbons (nitro-PAHs) using molecular docking, MM-GBSA energy estimations, QSAR modeling, and in silico toxicity prediction. Our findings highlight that several nitro-PAHs, particularly dinitro-substituted compounds like 2,7-dinitropyrene, possess high DNA-binding affinities, suggesting a strong potential to form persistent adducts and disrupt genomic integrity. The Glide XP docking and MM-GBSA scoring consistently identified key structural features—such as extended π-conjugation, planar geometries, and polar functional groups—as critical drivers of ligand–DNA interactions. The developed QSAR model, particularly the multiple linear regression approach, demonstrated strong predictive capability even in a small-data regime, underscoring the relevance of carefully selected physicochemical descriptors, such as molecular surface area, polarizability, and Connolly surface metrics, in modeling DNA-binding propensities. Importantly, the in silico toxicity profiling corroborated the docking results, revealing widespread mutagenic potential and highlighting additional biological risks, including endocrine disruption and blood-brain barrier permeability. Taken together, this study underscores the utility of virtual

screening and predictive modeling in identifying hazardous nitro-PAHs and understanding their molecular mechanisms of toxicity. These insights contribute not only to the field of computational toxicology but also provide a valuable foundation for prioritizing compounds for further experimental validation, environmental monitoring, and regulatory assessment. It is essential to note that the current QSAR models were developed using a limited dataset of 12 compounds, which may limit their generalizability. Future work should therefore focus on expanding the chemical space by including larger and more structurally diverse nitro-PAHs, enabling broader predictive applicability. Moreover, this approach should be extended to diverse DNA targets to fully map the toxicological landscape of nitro-PAHs and related environmental pollutants.

Author Contributions

Conceptualization, A.B.; methodology, A.B.; software, A.B.; validation, A.B.; formal analysis, A.B.; investigation, A.B.; resources, A.B.; data curation, A.B.; writing—original draft preparation, A.B.; writing—review and editing, A.B.; visualization, A.B.; supervision, A.B.

Institutional Review Board Statement

Not applicable.

Informed Consent Statement

Not applicable.

Data Availability Statement

The data that support the findings of this study are available from the corresponding author, AB, upon reasonable request.

Funding

This research received no external funding.

Acknowledgments

This research has no acknowledgment.

Conflicts of Interest

The author declares no conflict of interest.

References

1. Abdel-Shafy, H.I.; Mansour, M.S.M. A Review on Polycyclic Aromatic Hydrocarbons: Source, Environmental Impact, Effect on Human Health and Remediation. *Egypt. J. Pet.* **2016**, *25*, 107–123, https://doi.org/10.1016/J.EJPE.2015.03.011.
2. Kim, K.H.; Jahan, S.A.; Kabir, E.; Brown, R.J.C. A Review of Airborne Polycyclic Aromatic Hydrocarbons (PAHs) and Their Human Health Effects. *Environ. Int.* **2013**, *60*, 71–80, https://doi.org/10.1016/J.ENVINT.2013.07.019.
3. Patel, A.B.; Polycyclic Aromatic Hydrocarbons: Sources, Toxicity, and Advanced Remediation Techniques. *Front. Microbiol.* **2020**, 11, 562813, https://doi.org/10.3389/fmicb.2020.562813.

4. Srogi, K. Monitoring of Environmental Exposure to Polycyclic Aromatic Hydrocarbons: A Review. *Environ. Chem. Lett.* **2007**, *5*, 169–195, https://doi.org/10.1007/S10311-007-0095-0.
5. Xie, W.; Wang, G.; Yu, E.; Xie, J.; Gong, W.; Li, Z.; Zhang, K.; Xia, Y.; Tian, J.; Li, H. Residue Character of Polycyclic Aromatic Hydrocarbons in River Aquatic Organisms Coupled with Geographic Distribution, Feeding Behavior, and Human Edible Risk. *Sci. Total Environ.* **2023**, *895*, 164814, https://doi.org/10.1016/J.SCITOTENV.2023.164814.
6. Gad, S.C.; Gad, S.E. Polycyclic Aromatic Hydrocarbons (PAHs). In Encyclopedia of Toxicology (Third Edition), Wexler, P., Ed.; Academic Press: Oxford, **2014**; pp. 1040-1042, https://doi.org/10.1016/B978-0-12-386454-3.00911-8.
7. Gaurav, G.K.; Mehmood, T.; Kumar, M.; Cheng, L.; Sathishkumar, K.; Kumar, A.; Yadav, D. Review on Polycyclic Aromatic Hydrocarbons (PAHs) Migration from Wastewater. *J. Contam. Hydrol.* **2021**, *236*, 103715, https://doi.org/10.1016/J.JCONHYD.2020.103715.
8. Fu, P.P.; Herreno-Saenz, D.; Von Tungeln, L.S.; Lay, J.O.; Wu, Y.S.; Evans, F.E. DNA Adducts and Carcinogenicity of Nitro-Polycyclic Aromatic Hydrocarbons. *Environ. Health Perspect.* **1994**, *102*, 177-183, https://doi.org/10.1289/EHP.94102S6177.
9. Kriek, E.; Rojas, M.; Alexandrov, K.; Bartsch, H. Polycyclic Aromatic Hydrocarbon-DNA Adducts in Humans: Relevance as Biomarkers for Exposure and Cancer Risk. *Mutat. Res. Mol. Mech. Mutagen.* **1998**, *400*, 215–231, https://doi.org/10.1016/S0027-5107(98)00065-7.
10. Ewa, B.; Danuta, M.Š. Polycyclic Aromatic Hydrocarbons and PAH-Related DNA Adducts. *J. Appl. Genet.* **2016**, *58*, 321-330, https://doi.org/10.1007/S13353-016-0380-3.
11. Nebert, D.W.; Dalton, T.P. The Role of Cytochrome P450 Enzymes in Endogenous Signalling Pathways and Environmental Carcinogenesis. *Nat. Rev. Cancer* **2006**, *6*, 947–960, https://doi.org/10.1038/nrc2015.
12. Adam, M.; Chaubah, L.; Bontes, B.W.; Mulachelah, N.A.; Veteran, J.; East, M.; Indonesia, J. Molecular Docking of Polycyclic Aromatic Hydrocarbons as Potentially Carcinogenic Molecules Through Binding with Aryl Hydrocarbon Receptor. *JSMARTech J. Smart Bioprospecting Technol.* **2019**, *1*, 12–15, https://doi.org/10.21776/UB.JSMARTECH.2019.001.01.3.
13. Bukowska, B.; Mokra, K.; Michałowicz, J. Benzo[a]Pyrene—Environmental Occurrence, Human Exposure, and Mechanisms of Toxicity. *Int. J. Mol. Sci.* **2022**, *23*, 6348, https://doi.org/10.3390/IJMS23116348.
14. Dat, N.D.; Chang, M.B. Review on Characteristics of PAHs in Atmosphere, Anthropogenic Sources and Control Technologies. *Sci. Total Environ.* **2017**, *609*, 682–693, https://doi.org/10.1016/J.SCITOTENV.2017.07.204.
15. Bandowe, B.A.M.; Meusel, H. Nitrated Polycyclic Aromatic Hydrocarbons (Nitro-PAHs) in the Environment – A Review. *Sci. Total Environ.* **2017**, *581–582*, 237–257, https://doi.org/10.1016/J.SCITOTENV.2016.12.115.
16. Femi-Oloye, O.P.; Sutton, R.T.; Gordon, H.D.; Ain Das, A.; Morenikeji, G.O.; Odorisio, M.K.; Francestscu, O.D.; Myers, R.L.; Oloye, F.F. An Assessment of Polycyclic Aromatic Hydrocarbons Using Estimation Programs. *Toxics* **2024**, *12*, 592, https://doi.org/10.3390/TOXICS12080592.
17. Jin, L.; Chen, B.; Ma, G.; Wei, X.; Yu, H. Molecular Interactions Governing the Rat Aryl Hydrocarbon Receptor Activities of Polycyclic Aromatic Compounds and Predictive Model Development. *Molecules* **2024**, *29*, 4619, https://doi.org/10.3390/molecules29194619.
18. Guo, Y.; Wang, Z.; Hou, C.; Li, H.; Chen, W.; Li, H.; Chen, H.; Shi, L. Remediation of Polycyclic Aromatic Hydrocarbon-Contaminated Soil Using Microwave-Activated Persulfate Oxidation System. *Sustainability* **2025**, *17*, 4897, https://doi.org/10.3390/SU17114897.
19. Liu, X.; Kanchana-At, T.; Trivitayanurak, W.; Chy, S.; Bordeerat, N.K. Particulate-Bound Polycyclic Aromatic Hydrocarbons and Heavy Metals in Indoor Air Collected from Religious Places for Human Health Risk Assessment. *Atmosphere* **2025**, *16*, 678, https://doi.org/10.3390/ATMOS16060678.
20. Saraga, D.E.; Wang, W.-N.; Hayakawa, K. Recent Research Progress on Nitropolycyclic Aromatic Hydrocarbons in Outdoor and Indoor Environments. *Appl. Sci.* **2022**, *12*, 11259, https://doi.org/10.3390/APP122111259.
21. Siangcham, T.; Vivithanaporn, P.; Jantakee, K.; Ruangtong, J.; Thongsepee, N.; Martviset, P.; Chantree, P.; Sornchuer, P.; Sangpairoj, K. Impact of Benzo(a)Pyrene and Pyrene Exposure on Activating Autophagy and Correlation with Endoplasmic Reticulum Stress in Human Astrocytes. *Int. J. Mol. Sci.* **2025**, *26*, 1748, https://doi.org/10.3390/IJMS26041748.
22. Huang, J.; Zhou, C.; Song, F.; Li, T.; Wang, J.; Fu, X. Environmental DNA-Based Ecological Risk Assessment of PAHs in Aged Petroleum-Contaminated Soils. *Toxics* **2025**, *13*, 357,

https://doi.org/10.3390/TOXICS13050357.
23. Gomaa, M.S.; Alturki, M.S.; Tawfeeq, N.; Hussein, D.A.; Pottoo, F.H.; Al Khzem, A.H.; Sarafroz, M.; Abubshait, S. Discovery of Non-Peptide GLP-1 Positive Allosteric Modulators from Natural Products: Virtual Screening, Molecular Dynamics, ADMET Profiling, Repurposing, and Chemical Scaffolds Identification. *Pharmaceutics* **2024**, *16*, 1607, https://doi.org/10.3390/pharmaceutics16121607.
24. Mohamed, M.S.; Elsaman, T.; Mohamed, M.A.; Eltayib, E.M.; Abdalla, A.E.; Idriss, M.T. Identification of Bacterial Oligopeptidase B Inhibitors from Microbial Natural Products: Molecular Insights, Docking Studies, MD Simulations, and ADMET Predictions. *Pharmaceuticals* **2025**, *18*, 709, https://doi.org/10.3390/ph18050709.
25. Akbariqomi, M.; Badri, T.; Mohammadi, M.; Sehri, S.Y.; Farnoosh, G. Enhancement of the Activity of Organophosphorus Hydrolase (OPH): An in Silico Approach Using Docking, Molecular Dynamics Simulation, and MM-PBSA. *Biointerface Res. Appl. Chem.* **2024**, *14*, 121, https://doi.org/10.33263/BRIAC145.121.
26. Barrado, A.I.; García, S.; Castrillejo, Y.; Barrado, E. Exploratory Data Analysis of PAH, Nitro-PAH and Hydroxy-PAH Concentrations in Atmospheric PM10-Bound Aerosol Particles. Correlations with Physical and Chemical Factors. *Atmos. Environ.* **2013**, *67*, 385–393, https://doi.org/10.1016/J.ATMOSENV.2012.10.030.
27. Montano, L.; Baldini, G.M.; Piscopo, M.; Liguori, G.; Lombardi, R.; Ricciardi, M.; Esposito, G.; Pinto, G.; Fontanarosa, C.; Spinelli, M. Polycyclic Aromatic Hydrocarbons (PAHs) in the Environment: Occupational Exposure, Health Risks and Fertility Implications. *Toxics* **2025**, *13*, 151, https://doi.org/10.3390/TOXICS13030151.
28. Vondráček, J.; Machala, M. The Role of Metabolism in Toxicity of Polycyclic Aromatic Hydrocarbons and Their Non-Genotoxic Modes of Action. *Curr. Drug Metab.* **2021**, *22*, 584–595, https://doi.org/10.2174/1389200221999201125205725.
29. Lee, Y.Y.; Hsieh, Y.K.; Huang, B.W.; Mutuku, J.K.; Chang-Chien, G.P.; Huang, S. An Overview: PAH and Nitro-PAH Emission from the Stationary Sources and Their Transformations in the Atmosphere. *Aerosol Air Qual. Res.* **2022**, *22*, 220164, https://doi.org/10.4209/aaqr.220164.
30. Bieler, C.A.; Wiessler, M.; Erdinger, L.; Suzuki, H.; Enya, T.; Schmeiser, H.H. DNA Adduct Formation from the Mutagenic Air Pollutant 3-Nitrobenzanthrone. *Mutat. Res. Toxicol. Environ. Mutagen.* **1999**, *439*, 307–311, https://doi.org/10.1016/S1383-5718(98)00197-1.
31. Gadkari, V.V.; Tokarsky, E.J.; Malik, C.K.; Basu, A.K.; Suo, Z. Mechanistic Investigation of the Bypass of a Bulky Aromatic DNA Adduct Catalyzed by a Y-Family DNA Polymerase. *DNA Repair* **2014**, *21*, 65–77, https://doi.org/10.1016/J.DNAREP.2014.06.003.
32. Arlt, V.M.; Glatt, H.; da Costa, G.G.; Reynisson, J.; Takamura-Enya, T.; Phillips, D.H. Mutagenicity and DNA Adduct Formation by the Urban Air Pollutant 2-Nitrobenzanthrone. *Toxicol. Sci.* **2007**, *98*, 445–457, https://doi.org/10.1093/TOXSCI/KFM103.
33. Brown, D.G.; Sanderson, M.R.; Garman, E.; Neidle, S. Crystal Structure of a Berenil-d(CGCAAATTTGCG) Complex: An Example of Drug-DNA Recognition Based on Sequence-Dependent Structural Features. *J. Mol. Biol.* **1992**, *226*, 481–490, https://doi.org/10.1016/0022-2836(92)90962-J.
34. Cao, W.; Yuan, J.; Geng, S.; Zou, J.; Dou, J.; Fan, F. Oxygenated and Nitrated Polycyclic Aromatic Hydrocarbons: Sources, Quantification, Incidence, Toxicity, and Fate in Soil - A Review Study. *Processes* **2023,** 11, 52, https://doi.org/10.3390/pr11010052.
35. Sander, T.; Freyss, J.; Von Korff, M.; Rufener, C. DataWarrior: An Open-Source Program for Chemistry Aware Data Visualization and Analysis. *J. Chem. Inf. Model.* **2015**, *55*, 460–473, https://doi.org/10.1021/ci500588j.
36. Zhang, T.; Sun, G.; Cheng, X.; Cao, C.; Cai, Z.; Zhou, J. Screening for Potential Antiviral Compounds from Cyanobacterial Secondary Metabolites Using Machine Learning. *Mar. Drugs* **2024**, *22*, 501, https://doi.org/10.3390/MD22110501.
37. Buccheri, R.; Coco, A.; Pasquinucci, L.; Amata, E.; Marrazzo, A.; Rescifina, A. Enhancing HDAC Inhibitor Screening: Addressing Zinc Parameterization and Ligand Protonation in Docking Studies. *Int. J. Mol. Sci.* **2025**, *26*, 850, https://doi.org/10.3390/ijms26020850.
38. Di Spirito, F.; Veg, E.; Hashmi, K.; Joshi, S.; Khan, T. Computational Drug-Likeness Studies of Selected Thiosemicarbazones: A Sustainable Approach for Drug Designing. *Eng. Proc.* **2025**, *87*, 35, https://doi.org/10.3390/ENGPROC2025087035.
39. Ali, M.A.; Sheikh, H.; Yaseen, M.; Faruqe, M.O.; Ullah, I.; Kumar, N.; Bhat, M.A.; Mollah, M.N.H.

Exploring the Therapeutic Potential of Petiveria Alliacea L. Phytochemicals: A Computational Study on Inhibiting SARS-CoV-2's Main Protease (Mpro). *Molecules* **2024**, *29*, 2524, https://doi.org/10.3390/molecules29112524.
40. Lin, S.; Tang, R.W.L.; Ye, Y.; Xia, C.; Wu, J.; Duan, R.; Leung, K.W.; Dong, T.T.X.; Tsim, K.W.K. Drug Screening of Flavonoids as Potential VEGF Inhibitors Through Computational Docking and Cell Models. *Molecules* **2025**, *30*, 257, https://doi.org/10.3390/molecules30020257.
41. Godschalk, F.; Genheden, S.; Söderhjelm, P.; Ryde, U. Comparison of MM/GBSA Calculations Based on Explicit and Implicit Solvent Simulations. *Phys. Chem. Chem. Phys.* **2013**, *15*, 7731–7739, https://doi.org/10.1039/C3CP00116D.
42. Genheden, S.; Ryde, U. The MM/PBSA and MM/GBSA Methods to Estimate Ligand-Binding Affinities. *Expert Opin. Drug Discov.* **2015**, *10*, 449-461, https://doi.org/10.1517/17460441.2015.1032936.
43. Pedregosa, F.; Varoquaux, G.; Gramfort, A.; Michel, V.; Thirion, B.; Grisel, O.; Blondel, M.; Prettenhofer, P.; Weiss, R.; Dubourg, V. Scikit-learn: Machine learning in Python. *J. Mach. Learn. Res.* **2011**, *12*, 2825-2830.
44. Santiago, C.B.; Guo, J.Y.; Sigman, M.S. Predictive and Mechanistic Multivariate Linear Regression Models for Reaction Development. *Chem. Sci.* **2018**, *9*, 2398–2412, https://doi.org/10.1039/C7SC04679K.
45. Conesa, A.; Hernández, R. Chapter 16 - Omics Data Integration in Systems Biology: Methods and Applications. In Comprehensive Analytical Chemistry, García-Cañas, V., Cifuentes, A., Simó, C., Eds.; Elsevier: **2014**; Volume 64, pp. 441-459, https://doi.org/10.1016/B978-0-444-62650-9.00016-6.
46. Fattouche, M.; Belaidi, S.; Abchir, O.; Al-Shaar, W.; Younes, K.; Al-Mogren, M.M.; Chtita, S.; Soualmia, F.; Hochlaf, M. ANN-QSAR, Molecular Docking, ADMET Predictions, and Molecular Dynamics Studies of Isothiazole Derivatives to Design New and Selective Inhibitors of HCV Polymerase NS5B. *Pharmaceuticals* **2024**, *17*, 1712, https://doi.org/10.3390/ph17121712.
47. Khedraoui, M.; Abchir, O.; Nour, H.; Yamari, I.; Errougui, A.; Samadi, A.; Chtita, S. An In Silico Study Based on QSAR and Molecular Docking and Molecular Dynamics Simulation for the Discovery of Novel Potent Inhibitor against AChE. *Pharmaceuticals* **2024**, *17*, 830, https://doi.org/10.3390/PH17070830.
48. Crocetti, L.; Giovannoni, M.P.; Pavlov, T.S.; Ivanov, V.; Melani, F.; Guerrini, G. Synthesis of 3-Carboxy-6-Sulfamoylquinolones and Mefloquine-Based Compounds as Panx1 Blockers: Molecular Docking, Electrophysiological and Cell Culture Studies. *Molecules* **2025**, *30*, 2171, https://doi.org/10.3390/molecules30102171.
49. Banerjee, P.; Kemmler, E.; Dunkel, M.; Preissner, R. ProTox 3.0: A Webserver for the Prediction of Toxicity of Chemicals. *Nucleic Acids Res.* **2024**, *52*, W513–W520, https://doi.org/10.1093/NAR/GKAE303.
50. Watt, D.L.; Utzat, C.D.; Hilario, P.; Foti, J.J.; Shuck, S.C.; Taylor, J.S.; Hogue, B.A.; Basu, A.K.; Wang, Z. Mutagenicity of the 1-Nitropyrene–DNA Adduct N-(Deoxyguanosin-8-yl)-1-aminopyrene in Mammalian *Cells. Chem. Res. Toxicol.* **2007**, 20, 1658–1664, https://doi.org/10.1021/tx700131e.

Publisher's Note & Disclaimer